Journal homepage: http://gwse.iheg.org.cn

Research Article

Study on the strength deterioration characteristics and microscopic mechanisms of moraine soil under freeze-thaw cycles

Peng-fei Wang[1,2,3,4], Ming-li Li[1*], Ming Chang[1], Jun-lin Jiang[1], Fan Yang[5,6], Zhi-qiang Zuo[1]

[1] *State Key Laboratory of Geohazard Prevention and Geoenvironment Protection*, *Chengdu University of Technology*, *Chengdu* 610054, *China*.
[2] *Sichuan Geological Environment Survey and Research Center*, *Chengdu* 610081, *China*.
[3] *SiChuan Huadi Building Engineering CO*, *LTD*, *Chengdu* 610081, *China*.
[4] *Sichuan Province Engineering Technology Research Center of Geohazard Prevention*, *Chengdu* 610081, *China*.
[5] *Institute of Sichuan Metal Geology Survey*, *Chengdu* 611700, *China*.
[6] *Sichuan Shushui Geological Environment Research Co.*, *LTD*, *Chengdu* 611700, *China*.

Abstract: To investigate the strength degradation characteristics and microscopic damage mechanisms of moraine soil under hydro-thermo-mechanical coupling conditions, a series of X-ray Diffraction (XRD), standard triaxial testing, Scanning Electron Microscopy (SEM), and Nuclear Magnetic Resonance (NMR) experiments were conducted. The mechanical property degradation laws and evolution characteristics of the microscopic pore structure of moraine soil under Freeze-Thaw (F-T) conditions were revealed. After F-T cycles, the stress-strain curves of moraine soil showed a strain-softening trend. In the early stage of F-T cycles (0–5 cycles), the shear strength and elastic modulus exhibited damage rate of approximately 10.33% ± 0.8% and 16.60% ± 1.2%, respectively. In the later stage (10–20 cycles), the strength parameters fluctuated slightly and tended to stabilize. The number of F-T cycles was negatively exponentially correlated with cohesion, while showing only slight fluctuation in the internal friction angle, thereby extending the Mohr-Coulomb strength criterion for moraine soil under F-T cycles. The NMR experiments quantitatively characterized the evolution of the internal pore structure of moraine soil under F-T cycles. As the number of F-T cycles increased, fine and micro pores gradually expanded and merged due to the frost-heaving effect during the water-ice phase transition, forming larger pores. The proportion of large and medium pores increased to 59.55% ± 2.1% (N=20), while that of fine and micro pores decreased to 40.45% ± 2.1% (N=20). The evolution of pore structure characteristics was essentially completed in the later stage of F-T cycles (10–20 cycles). This study provides a theoretical foundation and technical support for major engineering construction and disaster prevention in the Qinghai-Xizang Plateau.

Keywords: Moraine soil in the Qinghai-Xizang Plateau; F-T cycle; Standard triaxial tests; soil strength degradation; Mohr-Coulomb criterion; Microscopic pore structure

Received: 15 Apr 2025/ Accepted: 09 Oct 2025/ Published: 25 Jan 2026

Introduction

The Qinghai-Xizang Plateau, known as the "Roof of the World," "Water Tower of Asia," and the "Third Pole," has been experiencing rapid glacier retreat under global warming, with perennial glacier and permafrost areas gradually transitioning into seasonal Frozone-Thawed (F-T) zones (Peng et al. 2022). Moraine soil, formed by the advance, transport, and deposition of glaciers during the Quaternary period (Wang et al. 2020; Lv et al. 2017), is widely distributed in seasonal frozen regions such as the Qinghai-Xizang Plateau and the western Sichuan Plateau in China (Cui et al. 2022; Allen et al. 2019; Liu et al. 2019; Ashraf

*Corresponding author: Ming-li Li, *E-mail address*: 784189855@qq.com

DOI: 10.26599/JGSE.2026.9280068

Wang PF, Li ML, Chang M, et al. 2026. Study on the strength deterioration characteristics and microscopic mechanisms of moraine soil under freeze-thaw cycles. Journal of Groundwater Science and Engineering, 14(1): 15-31.

et al. 2012). This soil type is characterized by poor particle sorting, lack of stratification, and a wide range of grain sizes (Guo et al. 2023; Zhou et al. 2023; Gao et al. 2019). Under the influence of global climate change, moraine soils are subject to frequent seasonal F-T cycles (Wang et al. 2023; Shen et al. 2022; Zhao et al. 2021; Liu et al. 2016), leading to significant degradation of their microstructure and mechanical strength (Chen et al. 2019a; Luo et al. 2019; Han et al. 2018). Such deterioration can trigger plateau geological hazards, including glacial lake outbursts, glacier debris flows, and ice-rock avalanches, posing serious risks to major infrastructure projects such as the Sichuan-Xizang Railway, hydraulic engineering works, tunnels, and highways (Jiang et al. 2024; Palamakumbura et al. 2021; Zhou et al. 2020; Chen et al. 2019b; Qu et al. 2018; KlimeŠ et al. 2016).

The results of large-scale direct shear tests showed that moraine soil possessed certain structural strength, attributed to the cementation and interlocking of coarse and fine particles (Neupane et al. 2019; Chen et al. 2019c). Once this structure was damaged under F-T cycles, it leds to the degradation of its strength propertiescs (Guo et al. 2022). The cohesion of moraine soil was found to be negatively correlated with the number of F-T cycles, while the internal friction angle fluctuated within a certain range, showing no clear relationship (Zhou et al. 2019). The initial water content was also a key factor governing changes in its physical and mechanical behavior. The initial water content influenced the water-ice phase transition process of moraine soil, promoting changes in the internal pore structure, thereby affecting its mechanical strength (Zhang et al. 2024; Feng et al. 2024). In terms of microscopic studies, Lebourg et al. (2004) used digital imaging technology to investigate the morphology and structural characteristics of moraine soil aggregates, while Sokolov et al. (2007) used SEM to reveal that the pore structure characteristics significantly change under the effect of F-T cycles. In summary, previous research concerning the property degradation of moraine soil under F-T cycles mainly focused on the changes in basic physical properties and conventional mechanical properties (such as uniaxial compressive strength), which has yielded valuable findings. However, previous studies have often omitted the effect of in-situ confining pressure, failed to explain the underlying microscopic mechanisms responsible for strength deterioration, and lacked quantitative analysis on the pore-structure evolution induced by F-T cycling.

In response to the major demands for disaster prevention and mitigation infrastructure development in the Qinghai-Xizang Plateau region, the study focused the impact of repeated F-T cycles on moraine soil in cold, high-altitude areas. It aimed to investigate the strength degradation mechanisms of moraine soil under coupled thermal-hydraulic-mechanical conditions. Using a combination of macro-microscopic geotechnical mechanical testing methods, including X-ray Diffraction (XRD), static triaxial testing system, SEM and NMR Popov's method, this study revealed the evolution of the mechanical properties of moraine soil under F-T cycles, including changes in the stress-strain relationships, elastic modulus, and shear strength. Additionally, it explored the microstructure evolution of the pore structure and particle arrangement of moraine soil under F-T cycles. This research provides theoretical support and parameter guidance for disaster prevention and mitigation, as well as for monitoring, early warning, and engineering construction in geologically fragile plateau regions, thereby contributing to the coordinated development of human-environment systems on the Qinghai-Xizang Plateau.

1 Materials and methods

1.1 The experimental materials

The experimental soil used in this study was collected from the field site in Nuque gully, located in Sangri County, Shannan City, Xizang Autonomous Region. The geographical coordinates of Nuque gully are between 29°13′–29°21′ N latitude and 92°18′–92°26′ E longitude, with an elevation range of 4,000–6,000 m. The basin has a leaf-like terrain, with a main stream length of approximately 17.8 km, an average slope of around 70 ‰, and a basin area of 64.5 km^2. According to field survey data, the study area exhibits glacier features such as glacial striations, glacially transported boulder, and sheep horn stones, supporting the identification of the region as a moraine soil landform.

To minimize disturbance to the moraine soil, intact soil columns were carefully excavated at the sampling location, placed in cubic containers with a side length of 20 cm, wrapped in cling film, and transported back to the laboratory. The basic physical property tests were conducted in accordance with the "GB/T 50123—2019 Standard for Soil Testing Methods", and the basic physical parameters of the moraine soil are presented in Table 1.

Table 1 The basic physical parameters of moraine soil

Dry density ρ_d/(g/cm^3)	Unit weight γ/(kN/m^3)	Optimum moisture content w_o/(%)	Maximum dry density $\rho_{d\max}$/(g/cm^3)	Nonuniform coefficient C_u	Curvature coefficient C_c
1.7	26.1	14.1%	2.30	2.20	0.94

The proportion of particles in the 0.25 mm–2 mm particle size range was 75.92% (>50%), classifying it as sand within the coarse-grained soil category. The content of particles smaller than 2 mm accounted for more than 70% of the total quality of the soil, meeting the requirements for the standard triaxial test. The uniformity coefficient (Cu) was 2.20, and the curvature coefficient (Cc) was 0.94. This moraine soil is poorly graded glacial sand, and the grading curve is shown in Fig. 1.

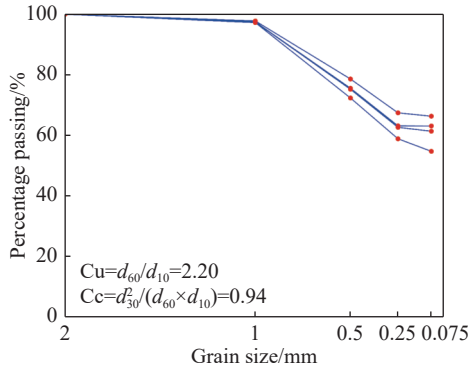

Fig. 1 The gradation curve of moraine soil

1.2 The test scheme

The main experiments include standard triaxial tests (sample dimensions: Φ50 mm×h100 mm), microscopic structural tests (XRD diffraction, NMR, and SEM) to investigate the cementation degree of moraine soil, the influence of F-T cycles on the strength characteristics of moraine soil samples, and the underlying microscopic mechanisms. Fang and Huang (2013) emphasized that the cementation of moraine soil was a key factor influencing its mechanical strength. Therefore, XRD diffraction tests were first conducted to explore the cementation of moraine soil.

To simulate the actual local temperature conditions during the F-T cycle tests, the average maximum and minimum monthly temperatures over the past five years in Shannan City were used. Each F-T cycle of the moraine soil lasted for 22 hours, with the soil frozen at −16°C for 11 hours and thawed at 28°C for 11 hours, and a heating/cooling rate of 4°C/h. After completing one F-T cycle, the samples were placed in a curing box and left to rest for 12 hours with a humidity set to 60%, consistent with field monitoring data, to facilitate water replenishment process.

For the indoor standard triaxial tests, experiments were conducted considering the initial moisture content and confining pressure on the samples after F-T cycles. The optimum moisture content of moraine soil was 14.1%, and the natural moisture content ranged from 6.11% to 11.51%, with an average initial moisture content of 10.7%. Thus, the moisture content for the standard triaxial tests was set near the optimum value, considering field conditions. Gradients of moisture content were set to 10.7%, 14.1%, and 18%. Given that the early stages of F-T cycles had a more significant effect on the strength properties of moraine soil (Pan et al. 2017), the F-T cycle counts were set to 0, 2, 5, 10, 15, and 20 cycles (Table 2).

The confining pressure was used to simulate the ground stress, which increased with the burial depth of moraine soil ($\sigma_3 = \gamma \cdot h$, where σ_3 is confining pressure, γ is unit weight, and h is burial depth). Based on the field conditions (h = 3.5–11.5 m), confining pressures for the indoor tests were set to 100 kPa, 150 kPa, and 200 kPa. The samples, compacted to 90% compaction degree and subjected to the required number of F-T cycles, were immediately placed into the standard triaxial system for Consolidation Undrained (CU) testing to simulate shear conditions in extreme

Table 2 The experimental scheme

Experiment name	Moisture Content w/%	Confining Pressure σ_3/kPa	Number of F-T Cycle N	Number of Samples
Consolidated undrained triaxial test (CU)	10.7 14.1 18	100，150，200	0，2，5，10，15，20	162
NMR	Moisture Content w/%		Number of F-T Cycle N	Number of Samples
	10.7		0，2，5，10，15，20	18
SEM	Moisture Content w/%	Magnification power	Number of F-T Cycle N	Number of Samples
	10.7	100×、200×	0，2，5，10，15，20	6

environments.

The tests followed the "GB/T 50123—2019 Standard for Soil Testing Methods" and applied axial compression at a shear rate of 0.8 mm/min, continuing until the axial strain reached 20%. To ensure the reliability of the results, each unique set of testing conditions (i.e., a specific combination of water content, confining pressure, and number of F-T cycles) was replicated three times (n=3), resulting in a total of 3 (water contents) × 3 (confining pressures) × 6 (F-T cycles) × 3 (replicates) = 162 standard triaxial tests. The flowchart of the experimental procedure is shown in Fig. 2.

The NMR tests were conducted using the MacroMR12-150H-I large-aperture nuclear magnetic resonance analysis and imaging system, with a magnetic field strength of 0.3 T. The T2 relaxation time test range was set from 0.1 ms to 1,000 ms to comprehensively cover the pore size distribution of moraine soil, from micropores to macropores. For each F-T cycle condition and moisture content level, three parallel samples were prepared, resulting in a total of 18 samples, ensuring experimental repeatability.

The SEM tests were performed using the Prisma E SEM scanning electron microscope. Prior to the SEM experiments, the F-T cycled samples were cut into thin slices with dimensions of 0.5 cm × 0.5 cm × 0.3 cm, followed by vacuum drying to remove moisture. Subsequently, the samples were subjected to gold sputtering to enhance conductivity before observation. For SEM observation, magnifications of 100× and 200× were selected, based on the particle size of glacial moraine soil and the scale of pore evolution.

2 The experimental results and analyses

This section comprehensively presents the experimental results and analyses of moraine soil under F-T cycles, integrating macro-mechanical properties with microstructural evolution. The findings are derived from a multi-technique approach, including XRD to determine mineral composition and evaluate the degree of cementation, standard triaxial tests to examine stress-strain behavior and quantify strength parameters, SEM for qualitative

Fig. 2 The flowchart diagram of the experimental procedure

microstructural observation, and NMR to quantitatively analyze pore structure characteristics. These results collectively reveal the laws governing mechanical property deterioration of moraine soil, linking microscopic changes to macroscopic mechanical property degradation.

2.1 The XRD tests

The experiment soil particles were classified as coarse-grained soil and the Bruker D8 Advance X-ray powder diffraction (XRD) instrument was used to analyze the degree of cementation. The test angle range was 5° to 40°, with the scanning speed of 5°/min. The XRD diffraction pattern showed that the moraine soil had weak cementation, primarily siliceous cementing agent. The mineral composition of the moraine soil included quartz, sodium feldspar, orthoclase, hornblende, muscovite, and a small amount of chlorite (Fig. 3).

2.2 The standard triaxial tests

2.2.1 The stress-strain relationship of moraine Soil

Figs. 4 present the stress-strain relationship curves of moraine soil under different initial moisture contents (10.7%, 14.1%, 18%), different confining pressures (100 kPa, 150 kPa, 200 kPa), and various numbers of F-T cycles. The stress-strain relationship curves at different initial moisture contents under various confining pressures generally exhibited a strain-softening trend. As strain increased, the stress of moraine soil initially rose rapidly, but after reaching a certain strain value, the stress began to decrease gradually. Under the fixed confining pressure, as the number of F-T cycles increased, the stress-strain curves for moraine soil with different initial moisture contents shifted downward, approaching the strain axis. In the early stages of F-T cycles (when the number of F-T cycles N = 2), the decline in the stress-strain relationship curve was most pronounced. As the moisture content increased, the frost heave and thaw collapse effects of moraine soil became more significant, leading to more internal damage to the soil and a substantial reduction in its bearing capacity. As confining pressure increased, the stress-strain curve of moraine soil showed that, at the same strain, the higher axial stress needed to be applied to the sample, which was attributed to the "enclose-hoop" effect of the confining pressure on the soil sample.

2.2.2 The variation law of moraine soil elastic modulus

The elastic modulus is an important parameter to characterize the elastic properties of moraine soil. In the initial loading phase, the deformation of the soil approximated linear-elastic behavior. For ease of analysis, the deformation modulus of the tangent line in the linear elastic deformation phase was typically taken as the elastic modulus (Qiu et al. 2023). Currently, the elastic modulus was usually determined by fitting or drawing a secant line to the linear portion of the stress-strain curve during the initial loading phase, and the slope of this line was defined as the elastic modulus of the moraine soil sample. Since this method focused on the linear segment of the stress-strain curve, and the initial loading phase was considered as the linear elastic deformation phase, both the tangent and secant lay on approximately the same straight line. Therefore, in the early deformation stage ($\xi = 1$), the slope of the tangent could be considered as the elastic modulus (E) of moraine soil. During the initial loading phase, the relationship between stress and strain ($(\sigma_1 - \sigma_3) - \xi$) was essentially linear, and the ratio of the incremental of deviatoric stress to the incremental of axial strain

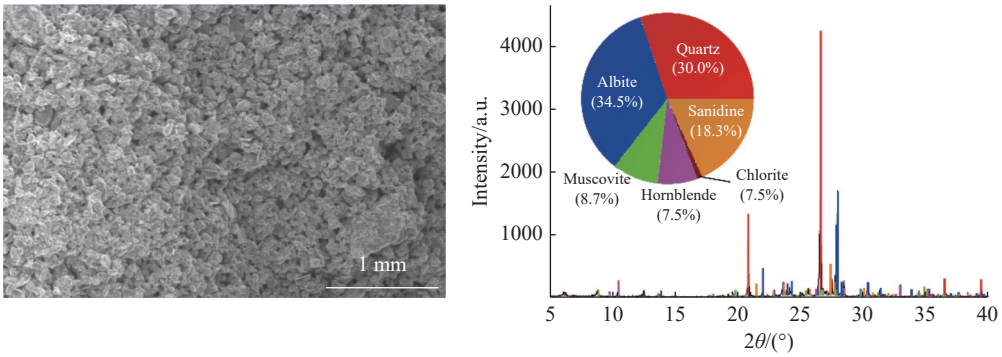

Fig. 3 Microstructure and mineral composition of the moraine soil. (a) SEM image of the soil sample (N=0 cycles, magnification: 200×); (b) XRD diffraction pattern identifying the primary mineral constituents, including quartz (Q), albite (A), orthoclase (O), hornblende (H), and muscovite (M)

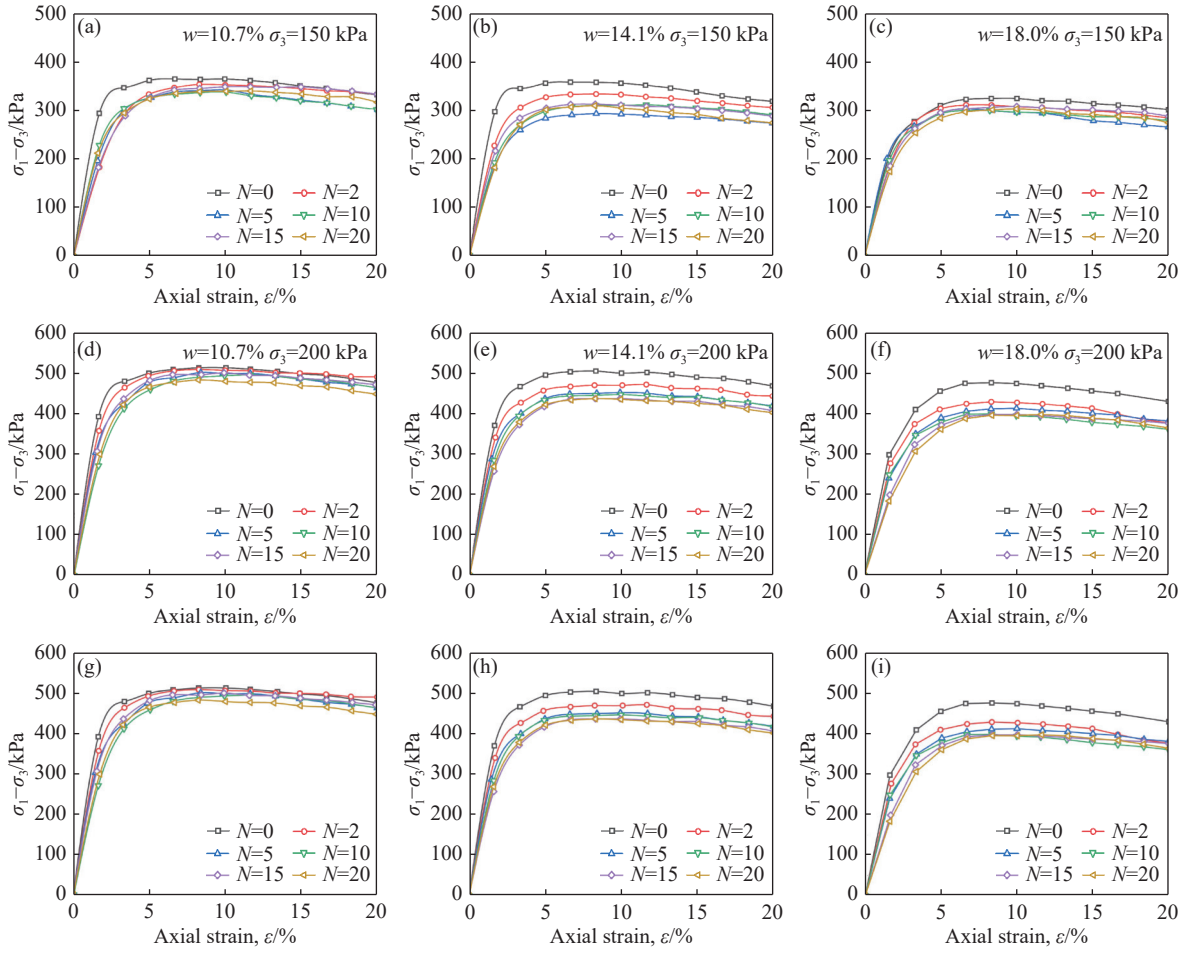

Fig. 4 The stress-strain curve of moraine under F-T cycle (a. σ_3 =100 kpa, w =10.7%, b. σ_3 =100 kpa, w =14.1%, c. σ_3 =100 kpa, w =18%, d. σ_3 =150 kpa, w =10.7%, e. σ_3 =150 kpa, w =14.1%, f. σ_3 =150 kpa, w =18%, g. σ_3 =200 kpa, w =10.7%, h. σ_3 =200 kpa, w =14.1%, i. σ_3 =200 kpa, w =18%)

could be used as the elastic modulus of the moraine soil:

$$E = \frac{\Delta\sigma}{\Delta\xi} = \frac{\sigma_{1.0\%} - \sigma_0}{\xi_{1.0\%} - \xi_0} \quad (1)$$

In the formula, E represents the elastic modulus of moraine soil (kPa), $\Delta\sigma$ denotes the incremental of deviatoric stress at $\xi = 1\%$ (kPa), and $\Delta\xi$ represents the incremental axial strain at strain $\xi = 1\%$ (%). The terms σ_0 and ξ_0 represent the initial deviatoric stress (kPa) and initial strain (%) of the secant line segment. Since no deformation occurred during the initial linear deformation phase, both σ_0 and ξ_0 were 0. From Equation (1), the elastic modulus curve of moraine soil under different conditions (i.e., varying initial moisture content, confining pressure, and number of F-T cycles) could be derived. Specifically, when ξ =1%, the ratio of the vertical and horizontal coordinates corresponded to the elastic modulus of the moraine soil.

As shown in Fig. 5, the elastic modulus decreased with increasing number of F-T cycles, indicating that the elastic characteristics of moraine soil were progressively weakened. Notably, in the early stages of F-T cycles (N = 0–5), the decrease in elastic modulus was especially significant, with the greatest elastic damage occurring in the soil. In the later stages of F-T cycles (N = 10–20), the elastic modulus declined slowly and showed a fluctuating trend. When confining pressure and the number of F-T cycles were held constant, the elastic modulus of moraine soil decreased with increasing moisture content. When the confining pressure increased to 200 kPa, the elastic modulus of moraine soil samples under all moisture content conditions increased, indicating that a larger elastic modulus corresponds to smaller compressive deformation under a given load, and increasing confining pressure enhances the bearing capacity of the soil.

The above research results demonstrate that under different confining pressures and initial moisture contents, the elastic modulus, a key

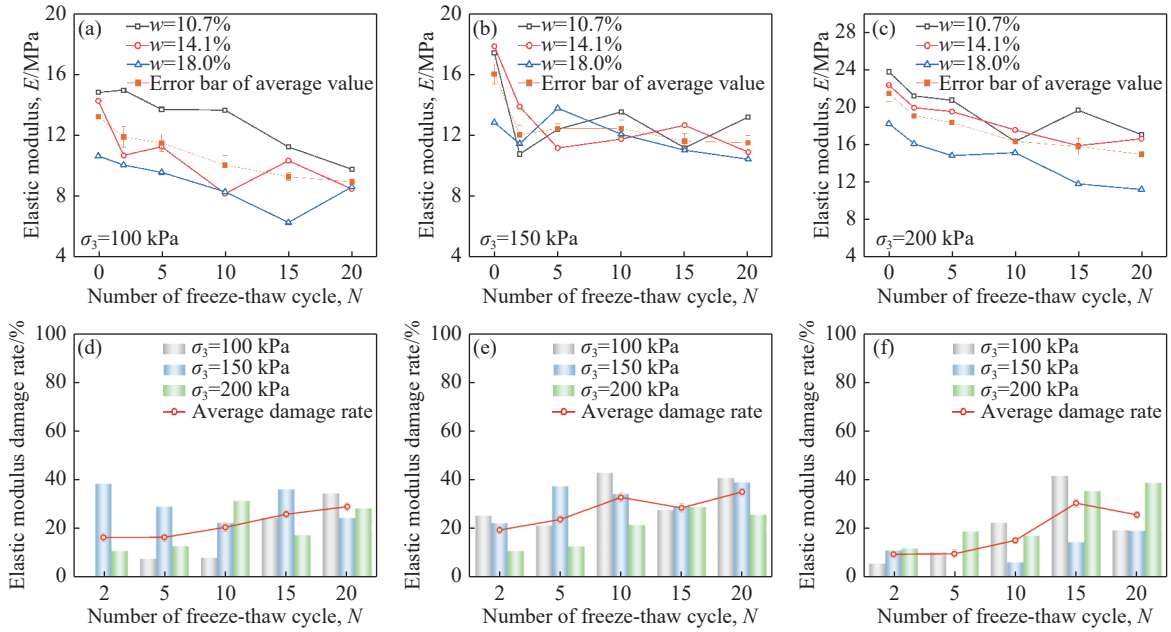

Fig. 5 The relationship between elastic modulus of moraine soil and number of F-T cycles (a. σ_3 =100 kpa, b. σ_3 =150 kpa, c. σ_3 =200 kpa, d. w =10.7%, e. w =14.1%, f. w =18%)

mechanical characteristic parameter of moraine soil, underwent significant degradation under the influence of F-T cycles. To further explore the effect of F-T cycles on the key mechanical parameters of the moraine soil, Lemaitre (1984) defined the damage rate of mechanical characteristic parameters, as follows:

$$K_I = 1 - \frac{I_N}{I_0} \tag{2}$$

In Equation (2), K represents the damage rate of the mechanical characteristic parameter, I refers to the important mechanical characteristic parameters of moraine soil (including elastic modulus E, shear strength τ_f, cohesion c, and internal friction angle φ), I_N represents the value of the mechanical characteristic parameter after N times F-T cycles, and I_0 represents the mechanical characteristic parameter value of moraine soil before F-T cycles. For the elastic modulus, the damage rate is: $K_E = 1 - \frac{E_N}{E_0}$.

As shown in Fig. 5, it was evident that with the increase in the number of F-T cycles, the average damage rate of the elastic modulus generally showed an increasing trend. When the initial moisture content was 10.7% and 14.1%, the average damage rate of the elastic modulus increased significantly during the early to mid-period of F-T cycles (N = 0–10). When the initial moisture content was 18%, the average damage rate of the elastic modulus increased significantly during the mid-period of F-T cycles (N = 5–10). Under the initial moisture content conditions of 10.7% and 14.1%, the maximum average damage rates of the elastic modulus reached 28.87% ± 2.1% and 38.97% ± 2.5%, respectively. As the initial moisture content increased, the average damage rate of the elastic modulus increased, indicating that a higher initial moisture content led to more free water and bound water in the soil, making it easier for the soil particles to move and weakening the soil's resistance to deformation. Additionally, when the confining pressure was 200 kPa, the damage rate of the elastic modulus was at its lowest. When the confining pressure was 100 kPa, the damage rate of the elastic modulus reached the highest values in several cases. Interestingly, the higher the confining pressure, the lower the damage rate, showing a negative correlation between the two. This was because the confining pressure induced a "enclose-hoop" effect, which increased the contact area between particles in the moraine soil and enhanced the ability of moraine soil to resist elastic deformation.

2.2.3 The variation law of shear strength of moraine soil under F-T cycle

The shear strength of moraine soil is one of the key indicators determining its strength. It not only affects the bearing capacity of the moraine soil but also influenced the stability of moraine dams during plateau glacial lake outburst disasters. From Figs. 4, it can be observed that after loading, the moraine soil initially exhibited a strain-softening behavior, followed by strain-hardening in the

middle and later stages of loading. The shear strength of moraine soil was taken as the deviator stress value $\sigma_1 - \sigma_3$ when strain hardening occurred at $\xi = 15\%$ in the later stages of loading.

The relationship between the shear strength of moraine soil and both confining pressure and F-T cycles is shown in Fig. 6. As the initial moisture content and confining pressure varied, the shear strength of moraine soil fluctuated slightly but generally showed a downward trend. Taking the optimal moisture content of 14.1% as an example, the shear strength of moraine soil under different graded confining pressures decreased by 15.28% ± 1.2%, 15.56% ± 1.3%, and 13.32% ± 1.1% after different numbers of F-T cycles, respectively. The decrease was most significant during the early F-T cycles (N = 0–5), and the shear strength gradually declined with a fluctuating trend in the later F-T cycles (N = 10–20). The above results indicate that when moraine soil was at the optimal moisture content, its shear strength decreased most sharply during the early F-T cycles (N = 0–5) and then showed minor fluctuations and tended to stabilize in the later cycles (N = 10–20). The trend of shear strength change under other initial moisture content conditions was similar to that observed under the optimal moisture condition.

The damage rate of shear strength was calculated as follows:

$$K_{\tau f} = 1 - \frac{\tau_{fN}}{\tau_{f0}} \tag{3}$$

Fig. 6 illustrates the relationship between shear strength and F-T cycle times for moraine soil under different confining pressures and initial moisture content conditions. The results showed that, under various moisture content conditions, during the early stage of F-T cycles (N = 0–5), the damage rate of shear strength increased sharply, followed by a slower rise accompanied by small fluctuations during the middle and later stages (N = 5–20). When the initial moisture content of the moraine soil reached the optimal moisture content of 14.1%, the maximum average damage rate reached 13.56% ± 1.0%, which was higher than that under lower initial moisture contents of w = 10.7% and w =18%. This was because at the optimal moisture content, the moraine soil achieved its maximum dry density, indicating the highest particle compactness, and therefore the damage caused by F-T cycles was most severe. The results of the confining pressure loading showed a negative correlation between confining pressure and the damage rate of shear strength—higher confining pressures resulted in slightly lower damage rates of shear strength (as shown by the green bars in the Fig. 6). For moraine soil in the Xizangan Plateau, it can be concluded that shallow-buried and surface moraine soils were more prone to shear strength damage, which explains why shallow landslides and moraine dam instability were more common in high-altitude regions, and why surface layers were more likely to experience dam break.

The elastic modulus serves as a key parameter for characterizing the elastic deformation charac-

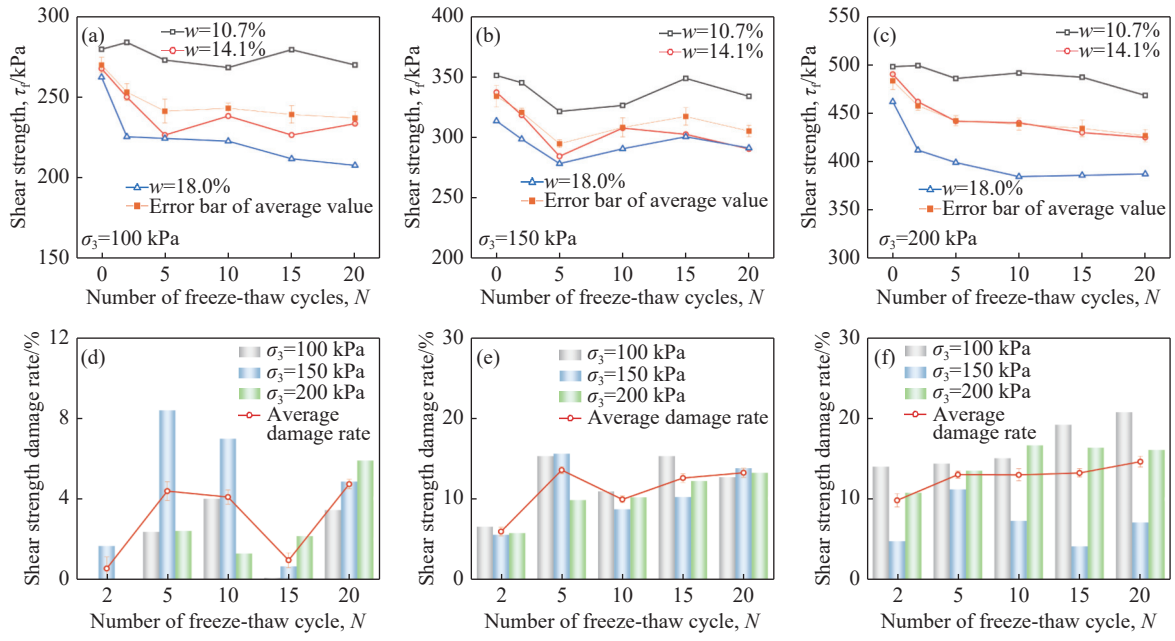

Fig. 6 The relationship between shear strength of moraine soil and number of F-T cycles (a. σ_3 =100 kpa, b. σ_3 =150 kpa, c. σ_3 =200 kpa, d. w =10.7%, e. w =14.1%, f. w =18%)

teristics of soil, while shear strength reflects the ability of soil to resist shear failure. Both parameters are crucial for evaluating the stability and bearing capacity of soil. However, in practical testing, shear strength typically requires field sampling followed by destructive techniques such as direct shear tests or triaxial tests. These methods are not only inconvenient for engineering measurement, but also infeasible for maintaining the original condition of the soil. On the other hand, the elastic modulus can be measured using non-destructive testing methods, such as ultrasonic testing, resonance frequency methods, and pulse velocity testing. Therefore, by establishing a relationship curve between the elastic modulus and shear strength of the moraine soil, the shear strength can be directly estimated from the elastic modulus measured in situ using non-destructive methods. As illustrated in Fig. 7, the relationship between the elastic modulus and the shear strength of moraine soil was positively correlated. In addition, the relationship showed only a weak dependence on F-T cycle times and the initial moisture content of the moraine soil. Thus, the relationship could be described using formula $\tau_f = 19.46E + 69.03$, with a correlation coefficient of 0.752. The majority of experimental results fell within the 95% confidence interval, indicating a strong correlation and satisfactory fitting performance.

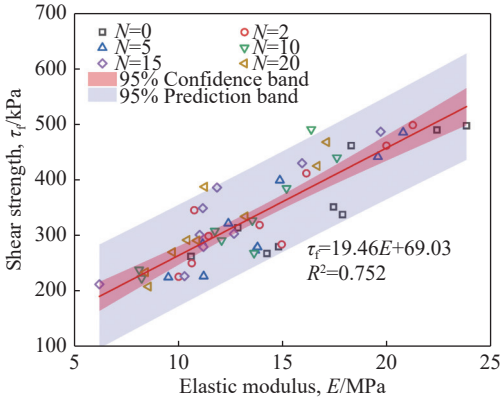

Fig. 7 The relationship curve between the elastic modulus and the shear strength

2.2.4 Variation law of the shear strength indices of moraine soil

Fig. 8 and Fig. 9 illustrate the relationship curves between F-T cycles, cohesion and internal friction angle of the moraine soil under different initial moisture content conditions. From top to bottom, the initial moisture content increased, and it can be observed that the moraine soil with higher initial moisture content had lower cohesion and internal friction angle compared to soil with lower initial

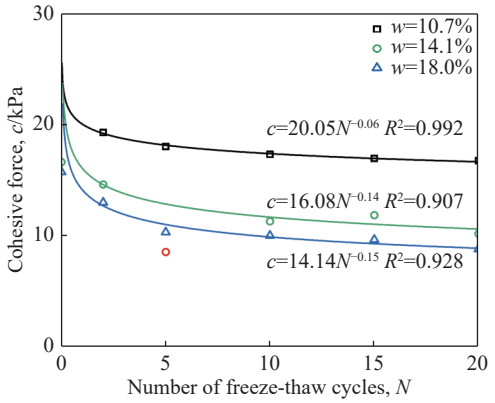

Fig. 8 The Relationship curve between the number of F-T cycles and cohesion

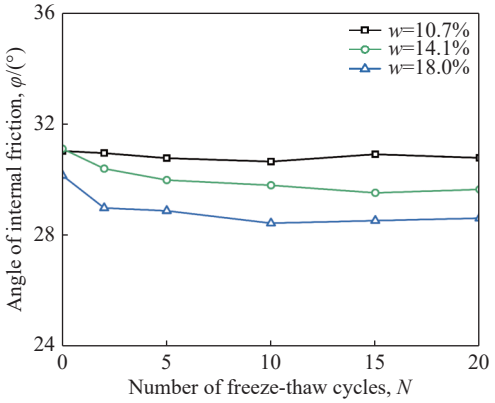

Fig. 9 The relationship curve between the number of F-T cycles and the angle of internal friction

moisture content. Under different initial moisture content conditions, the cohesion exhibited distinct variation patterns with increasing F-T cycles. In the early stage of F-T cycles (N = 0–5), cohesion decreased sharply, while in the later stages (N = 10–20), it declined more slowly and eventually stabilized. The internal friction angle decreased gradually and fluctuated within a narrow range. This indicated that the influence of F-T cycles on soil strength parameters was mainly reflected in the variation of cohesion. Therefore, a nonlinear fit between cohesion and the number of F-T cycles was performed, and the results revealed a negative exponential correlation between them, as expressed in Equitation (4).

$$c = aN^{-b} \tag{4}$$

In the formula, a and b denote fitting parameters, N represents the number of F-T cycles, and c is the cohesion of the moraine soil.

2.2.4.1 Mohr-Coulomb criterion expansion of the moraine soil under F-T cycle action

The above research results demonstrated that under

F-T cycles, the cohesion was strongly correlated with both the number of F-T cycles and the initial moisture content of the moraine soil, whereas the internal friction angle showed a weaker correlation with these parameters. Through numerical nonlinear regression analysis, a multi-parameter coupling mathematical model between cohesion c, initial moisture content (w), and F-T cycle number (N) was established. The Levenberg-Marquardt algorithm was applied to obtain the multi-parameter coupling model (Equation 5). Based on the classical Mohr-Coulomb criterion $\tau_f = c + \sigma \tan\varphi$, the results were further used to extend the criterion, thereby deriving a new Mohr-Coulomb strength criterion for moraine soil under F-T cycles (Equation 6).

$$c = 59.551 - 0.608N - 5.166w + 0.018N^2 + 0.147w^2 (R^2 = 0.960) \quad (5)$$

$$\tau_f = 59.551 - 0.608N - 5.166w + 0.018N^2 + 0.147w^2 + \sigma \tan\varphi \quad (6)$$

In the equation, τ_f represents the shear strength of the moraine soil, N is the number of F-T cycles, w is the moisture content of the moraine soil, σ is the normal stress on the failure plane, and φ is the internal friction angle of the moraine soil (Fig. 10). The goodness-of-fit of the extended Mohr-Coulomb model was thoroughly evaluated. The Levenberg-Marquardt algorithm yielded a high coefficient of determination ($R^2 = 0.942$) and a low root mean square error (RMSE = 12.45 kPa), indicating that the model effectively captures the relationship between the shear strength and the influencing factors (N, w, σ). Residual analysis revealed that the residuals were randomly distributed around zero, confirming the model's reliability and the absence of systematic bias. Therefore, the extended Mohr-Coulomb strength criterion can be applied to moraine soil with varying moisture contents under the influence of F-T cycles. Depending on the actual number of F-T cycles, this criterion can be used to evaluate shear strength under both seasonal and diurnal F-T cycles.

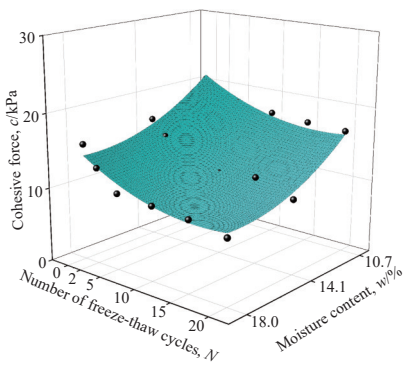

Fig. 10 The surface of relations between the number of F-T cycles and the cohesion force

2.2.4.2 The multi-parameter coupled modeling of mechanical characteristics of the moraine soil under F-T cycles

Shear strength, derived from the Mohr-Coulomb strength criterion, characterizes the soil's resistance to shear failure, while the elastic modulus serves as a key indicator of its elastic performance. Both parameters are significant for understanding the macroscopic mechanical properties of soil, such as stability and bearing capacity. The shear strength and elastic modulus of moraine soil are influenced by multiple factors, including initial moisture content, confining pressure, and the number of F-T cycles. Therefore, to explore the relationship between shear strength (τ_f), elastic modulus (E), and these influencing factors, a multi-parameter coupling model was developed. A numerical nonlinear regression analysis method was employed to establish the multi-parameter coupling mathematical model that relates shear strength (τ_f), elastic modulus (E), and the number of F-T cycles (N), using the Levenberg-Marquardt algorithm to achieve the optimal fitting. The relationships among shear strength (τ_f), elastic modulus (E), F-T cycle number (N), and initial moisture content (w) for moraine soil under a confining pressure of 300 kPa and at the optimal moisture content of 14.1% are expressed as follows:

$$\tau_f = \alpha_0 + \alpha_1 N + \alpha_2 w + \alpha_3 N^2 + \alpha_4 w^2 \quad (7)$$

$$E = \beta_0 + \beta_1 N + \beta_2 w + \beta_3 N^2 + \beta_4 w^2 \quad (8)$$

$$\tau_f = \chi_0 + \chi_1 N + \chi_2 \sigma_3 + \chi_3 N^2 + \chi_4 \sigma_3^2 \quad (9)$$

$$E = \delta_0 + \delta_1 N + \delta_2 \sigma_3 + \delta_3 N^2 + \delta_4 \sigma_3^2 \quad (10)$$

In the above equations, w represents the initial moisture content of the moraine soil, E is the elastic modulus (kPa). α_i, β_i, χ_i, and δ_i are the fitting parameters respectively. The nonlinear surface fitting results are shown in Fig. 11, with correlation coefficients of 0.915, 0.912, 0.987, and 0.928. All models achieved high R^2 values (exceeding 0.91) and low Root Mean Square Error (RMSE) values, demonstrating excellent fitting accuracy and predictive capability. The strong agreement between the predicted and experimental values confirms the effectiveness of the Levenberg-Marquardt algorithm in solving the nonlinear regression problems in this study.

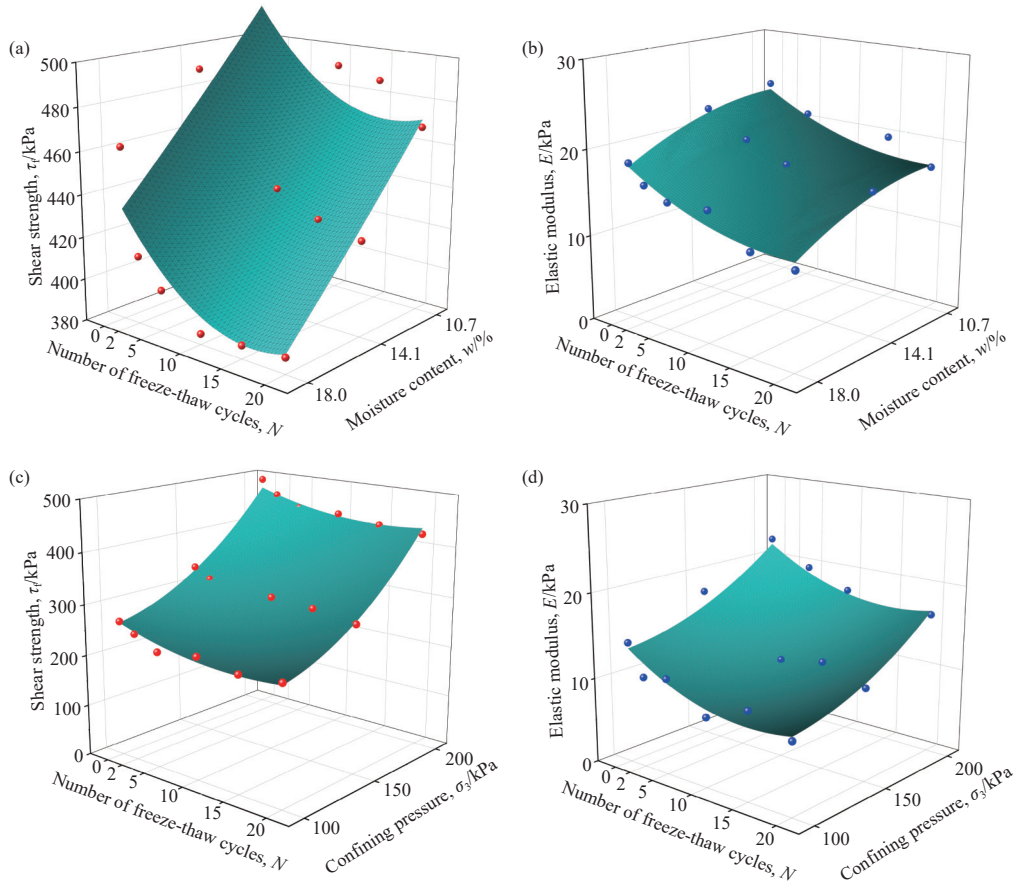

Fig. 11 The multi-parameter coupling model for mechanical characteristics of moraine soil (a. the relationship surface among shear strength, number of F-T cycles and initial moisture content, b. the relationship surface among elastic modulus, the number of F-T cycles and initial moisture content, c. the relationship surface among shear strength, number of F-T cycles and confining pressure, d. the relationship surface among elastic modulus, number of F-T cycles and confining pressure)

Under varying confining pressures, both the shear strength and elastic modulus of moraine soil decreased with the increase in F-T cycle number and moisture content. Additionally, both shear strength and elastic modulus decreased as the number of F-T cycles and confining pressure increased, with the trend being particularly pronounced in the early stage of F-T cycles. These research findings can provide reliable mechanical parameter references and support for engineering design in the Qinghai-Xizang Plateau, as well as for the prevention and control of plateau geological disasters.

2.3 The microscopic structure test results and analyses

2.3.1 The SEM results and qualitative analyses

To facilitate the observation of the impact of F-T cycles on microscopic structure of the moraine soil, SEM images of samples subjected to 0, 10, and 20 F-T cycles were taken at magnifications of 100× and 200×, as shown in Fig. 12. To quantitatively characterize the microstructural evolution, the SEM images were processed and analyzed using image analysis software. The key quantitative indicators, including porosity and average pore diameter, were statistically calculated. The analysis procedure included image binarization, noise removal, and particle/pore identification. The quantitative results are summarized in Table 3.

The quantitative data clearly demonstrate a significant increasing trend in both porosity and average pore diameter with the increasing number of F-T cycles. After 20 cycles, the porosity increased by 90.1% compared to the initial state (N=0), and the average pore diameter more than doubled. This quantitative trend objectively confirms the qualitative observation that F-T cycles cause the soil structure to loosen and pores to coarsen.

The moraine soil has undergone intense weathering due to prolonged exposure to F-T cycles,

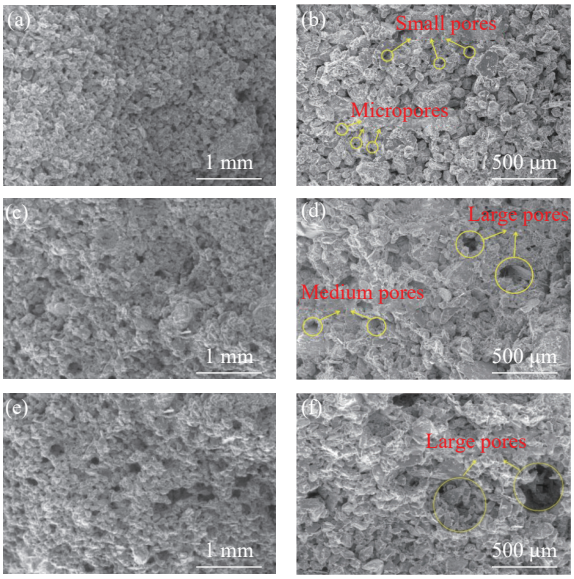

Fig. 12 The microstructure of moraine soil under different F-T cycles (a. *N*=0 and the magnification of 100×, b. *N*=0 and the magnification of 200×, c. *N*=10 and the magnification of 100×, d. *N*=10 and the magnification of 200×, e. *N*=20 and the magnification of 100×, f. *N*=20 and the magnification of 200×)

Table 3 Quantitative analysis of microstructure from SEM images

Number of F-T Cycles/N	Porosity/%	Average Pore Diameter/μm
0	15.2 ± 0.8	8.5 ± 0.5
10	22.7 ± 1.2	14.1 ± 0.7
20	28.9 ± 1.5	18.6 ± 0.9

resulting in relatively well-rounded particles. Qualitative analyses of the moraine soil microstructure were conducted. Before F-T cycles (Fig. 12(a) and Fig. 12 (b)), the SEM images clearly showed that the soil particles in the moraine soil were densely and orderly arranged, with a relatively stable soil structure. The pores in the soil were primarily micro and small-sized. After 10 F-T cycles (Fig. 12(c) and Fig. 12 (d)), the arrangement of the moraine soil particles began to shift from dense to looser state. The soil pores significantly increased in size compared to those before the F-T cycles. Additionally, in Fig. 12(d), large pores were observed, with clear signs of compression of the moraine soil particles around these pores. This was due to the frost heave effect caused by the phase transition of water into ice, which exerted pressure on the pore spaces and continuously compresses the soil, leading to changes in its microstructure and pore structure, resulting in a more loosely arranged particle distribution. After 20 F-T cycles (Fig. 12(e) and Fig. 12 (f)), the arrangement of the moraine soil particles became even looser. The soil pores further increased in size, and significantly larger pores were observed compared to after 10 F-T cycles. In Fig. 12(f), similar compression of the soil particles around the large pores was again evident. The frost heave stress caused further merging of the small pores, resulting in the formation of larger pores.

2.3.2 The test results of NMR

To further investigate the changes in the pore structure characteristics of moraine soil under F-T cycles, NMR experiments were conducted, focusing on the quantitative analyses of pore number and aperture distribution. Based on the average pore diameter, the pores can be classified into four categories: Micropores, small pores, mesopores, and macropores (Wang and Wang, 2000), with the pore sizes shown in Table 4. After processing the T2 relaxation times of the moraine soil samples subjected to different F-T cycles, the pore size distribution of moraine soil after various F-T cycles was summarized (Fig. 13). Additionally, the aperture distribution of the moraine soil after F-T cycles was statistically analyzed, resulting in the pore number proportion for different F-T cycle counts.

With the increase in the number of F-T cycles, the moraine soil samples generally exhibited a

Table 4 The pore classification table

The pore classification	Large pores	Medium pores	Small pores	Micropores
Size/μm	>100	100–30	30–3	<3

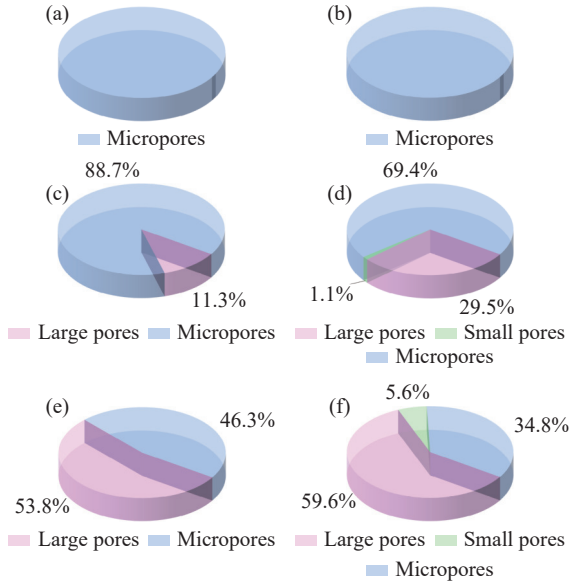

Fig. 13 The pore number ratio distribution diagram (a. *N*=0, b. *N*=2, c. *N*=5, d. *N*=10, e. *N*=15, f. *N*=20)

trend of increasing proportions of large and medium pores, while the proportions of micropores and small pores continuously decreased. For F-T cycles ranging from 2 to 20 (2, 5, 10, 15, 20), the proportions of large and medium pores increased from 0.00% to 11.33% ± 1.0%, 29.48% ± 1.8%, 53.75% ± 2.2%, and 59.55% ± 2.1%, respectively, while the proportion of micropores decreased from 100% to 88.67% ± 1.0%, 70.52% ± 1.8%, 40.25% ± 2.2%, and 40.45% ± 2.1%, respectively (Fig. 13). For F-T cycles from 0 to 2, the pore size distribution curve (Fig. 14) shifted to the right as the number of F-T cycles increased, indicating a general increase in pore size. Large and medium pores became more abundant, and soil particles were prone to displacement. The changes in the structural and pore characteristics of moraine soil led to a degradation in its strength properties. The evolution of pore characteristics occurred most rapidly in the early stage of F-T cycles (N=5), while in the later stage (N=10–20), the process gradually stabilized, and pore reorganization was nearly complete.

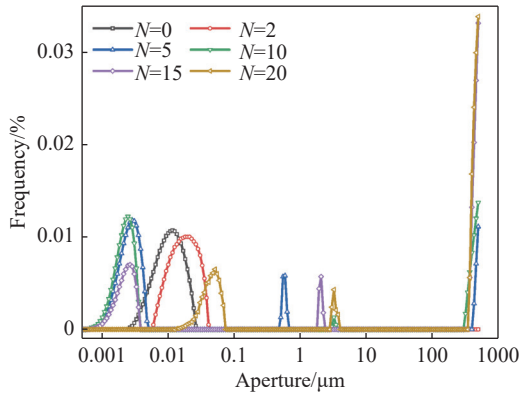

Fig. 14 The aperture distribution diagram

Based on NMR data, the pore fractal dimension (D_f) and average pore spacing (d_{avg}) were calculated to quantitatively analyze pore structure evolution under F-T cycles (Table 5). The fractal dimension was computed using a cumulative curve model based on T_2 relaxation time, while average pore spacing was estimated via porosity and equivalent pore number.

Table 5 Evolution of micro-pore structure parameters of moraine soil

N	Large-medium pore/%	D_f	d_{avg}
0	0.00	2.68±0.05	8.2±0.4
20	59.55±2.1	2.31±0.06	21.5±1.1

With increasing F-T cycles, the pore fractal dimension significantly decreased from 2.68 to 2.31, indicating that the pore structure evolved from a complex and irregular configuration to a simpler, more regular one. The average pore spacing increased from 8.2 μm to 21.5 μm, indicating a loosening of the soil structure. This directly correlates with macroscopic mechanical property degradation: the decrease in fractal dimension leads to reduction of cementing micro-pores and cohesion attenuation; the increase in pore spacing weakens soil stiffness and reduces elastic modulus. The most dramatic changes in microscopic parameters occurred in the early freeze-thaw stage (N=0–5), which aligns closedly with the staged characteristics of macroscopic mechanical damage.

The above results quantitatively analyzed the evolution process of the pore structure characteristics of moraine soil under F-T cycles. A comparative analyses with the degradation of strength characteristics in Section 3.2 revealed the relationship between the internal microstructure and macro strength. As the number of F-T cycles increased, the micropores and small pores in the moraine soil gradually merged and reorganized into large and medium pores. Large pores began to appear in the early stage of the F-T cycles (N=0–5), corresponding to the period when the stress-strain relationship and cohesion decreased most significantly, indicating the most prominent strength degradation. In the mid-stage of the F-T cycles (N=5–10), the small pores continued to merge into large and medium pores, with their proportion increasing to 29.48%. During this stage, the stress-strain relationship and cohesion continued to decline, showing persistent strength degradation. In the late stage of the F-T cycles (N=10–20), fine pores still merged and reorganized into large and medium pores, but the increase slowed down, with the proportion of large and medium pores increasing by only 5.80%. By this point, pore reorganization in the moraine soil was almost complete, and although the stress-strain curve and cohesion continued to decrease, the changes became gentler, indicating that the strength of the moraine soil was stabilizing. In summary, the evolution of the pore structure characteristics of moraine soil under F-T cycles on the Qinghai-Xizang Plateau closely corresponded to the observed degradation in its strength characteristics.

The mineralogical composition identified by XRD analysis in Section 3.1 provides a fundamental basis for understanding the mechanical response and microstructural evolution under F-T cycles. The dominance of quartz and feldspars, which are hard and non-expansive minerals, contributes to the high initial frictional strength and the strain-softening behavior observed in the triaxial tests.

More importantly, the weak siliceous cementation implies that the bonding between soil particles is inherently vulnerable. During F-T cycles, the frost heaving pressure generated by water-ice phase transition primarily targets these weak cementation points. The lack of strong clay minerals (e.g., montmorillonite) that could absorb water and swell means that the damage mechanism is predominantly mechanical, driven by the expansion of ice lenses within the pores. This accounts for the most significant degradation of cohesion and elastic modulus during the early F-T stages (N=0–5), when weak cementation is rapidly disrupted. The subsequent stabilization in later cycles (N=10–20) suggests that once the initial cementation is destroyed, the soil skeleton reorganizes into a relatively stable structure dominated by particle rearrangement and pore redistribution, as quantified by the NMR results.

3 Discussion

In the context of global warming, the continuous retreat of glaciers caused the permafrost moraine in the original moraine landform to begin to be subjected to seasonal F-T cycles, and its mechanical properties continued to deteriorate, thus affecting the stability of moraine dam, debris slope, etc., resulting in frequent geological disasters on the plateau such as glacial lake outburst debris flow. In this study, the standard indoor triaxial experiment method was first adopted. After field sampling, the variation patterns of key mechanical parameters (cohesion force and internal friction angle) of moraine soil under different confining pressure and initial moisture contents were systematically characterized with respect to the number of F-T cycles. The Mohr-Coulomb criterion for the moraine soil under F-T cycles was extended according to the experimental results. Subsequently, NMR and SEM experiments were carried out to qualitatively and quantitatively study the distribution and evolution characteristics of the moraine soil pore structure under different F-T cycles, and to find out the microscopic mechanism of the deterioration of the mechanical properties of the moraine soil.

The observed 15.28% ± 1.2% decrease in shear strength corresponds to an approximately 29.48% ± 1.8% increase in the proportion of large and medium pores (from 0% to 29.48%) and a 7.5% ± 0.5% increase in overall porosity. This establishes a direct and quantitative link between microstructural changes and macro-scale strength degradation. The underlying microscopic mechanism for the attenuation of mechanical parameters is that the increase in porosity and the coarsening of pores reduce the effective contact area between soil particles and weaken particle cementation, resulting in a decrease in bonding force (manifested as reduced cohesion) and a diminished ability of the soil to resist deformation (manifested as a decrease in elastic modulus) .

While the extended Mohr-Coulomb criterion and the multi-parameter coupling model effectively capture the strength degradation of moraine soil under the tested hydro-thermo-mechanical conditions, their applicability to complex, real-world engineering scenarios requires careful evaluation and additional validation. A primary limitation of the current study is that the constitutive models were derived from Conventional Triaxial Compression (CTC) tests under Consolidated Undrained (CU) conditions. This specific stress path, while fundamental, may not fully represent the complex, multi-directional loading and unloading cycles that slope moraine soil or moraine dam materials experience in situ. For example, stress paths encountered during an earthquake (cyclic loading), rapid excavation (unloading), or progressive slope failure can differ substantially from the monotonically increasing axial stress applied in laboratory tests. Consequently, the models' performance under such non-standard stress paths (e.g., reduced triaxial compression, cyclic loading, or stress rotation) remains unverified. This study primarily addresses static characteristics, while the dynamic response of moraine soil under the coupled effects of seismic dynamic loading and F-T cycles represents a critical area for future research. Furthermore, the fixed gradients of moisture content and confining pressure used in this study may not comprehensively capture the heterogeneous in-situ conditions of moraine soil across the Qinghai-Xizang Plateau. Potential influences of chemical components, such as salt and organic matter, on frost heaving and deterioration processes were also not considered, which may limit the direct applicability of these conclusions to all field scenarios.

In the future, numerical simulation methods can be further applied to reproduce the triaxial compression tests by using particle flow software PFC^{2D}. By combining these simulations with the comparative analysis of the laboratory test results presented above, the evolution of micro-cracks, displacement field and force chain field can be more thoroughly investigated, particularly after F-T cycling. Regarding the study of mechanical property deterioration of moraine under F-T cycle,

the research group plans to conduct dynamic triaxial tests and complementary numerical simulations to explore the dynamic characteristics of moraine soil. This includes examining the evolution of dynamic stress-dynamic strain curve and dynamic mechanical parameters, such as dynamic shear modulus, dynamic shear strength and damping ratio.

Such research will provide reliable dynamic and static mechanical parameters for engineering design involving Xizangan Plateau moraine, ensuring the safe construction and operation of major projects in cold, high-altitude environments. Furthermore, it will establish a theoretical foundation for better understanding plateau geological hazards associated with the deterioration of moraine strength and mechanical properties. The results of this study are expected to offer practical guidance and theoretical support for the prevention and control of major engineering projects (such as the Sichuan-Xizang Railway and highway tunnels) and geological hazards (e.g., glacial lake failures and debris flows) on the Qinghai-Xizang Plateau.

4 Conclusions

This study investigated the strength degradation characteristics of moraine soil on the Qinghai-Xizang Plateau under varying initial moisture contents and F-T cycles using standard triaxial tests, SEM tests, and NMR tests. The micro-mechanism underlying the degradation of soil properties were clarified. The main conclusions are summarized as follows:

(1) The stress-strain relationship curve of moraine soil after F-T cycles exhibited a strain-softening trend. With increasing F-T cycles, the stress-strain curves progressively shifted toward the strain axis.

(2) Both shear strength and the elastic modulus were strongly influenced by the number of F-T cycles and initial moisture content, showing a clear decreasing trend. In the early stage of the F-T cycles (N=0–5), the damage rates reached 10.33% ± 0.8% for shear strength and 16.60% ± 1.2% for elastic modulus. In the later stage (N=10–20), the damage rates fluctuated slightly and tended to stabilize. Cohesion decreased following a negative exponential function with respect to the number of F-T cycles, while the internal friction angle showed only minor fluctuations.

(3) The Mohr-Coulomb criterion for moraine soil under F-T cycles was extended, and a multi-parameter coupling model linking shear strength, elastic modulus, and F-T cycles was successfully established.

(4) The pore structure of moraine soil underwent significant changes under F-T cycles. Soil particles transitioned from a dense, ordered arrangement to a looser, more disordered state. Small pores gradually merged and reorganized into larger pores due to frost heave effect. By the late stage of the F-T cycles (N=20), the proportion of small and micropores decreased to 40.45% ± 2.1%, indicating that pore structure evolution was nearly complete.

Acknowledgements

The authors gratefully acknowledge support from the National Natural Science Foundation of China (Grant Nos. 42107193, 42077245).

The research was supported by the Sichuan Science and Technology Program (2025YFNH0008, 2025YFNH0004); the State Key Laboratory of Geohazard Prevention and Geoenvironment Protection Independent Research Project (SKLGP2023Z006); and the Everest Scientific Research Program 2.0: Research on mechanism and control of glacial lake outburst chain catastrophe in Qinghai-Xizang Plateau based on man-earth coordination perspective.

References

Allen SK, Zhang GQ, Wang WC, et al. 2019. Potentially dangerous glacial lakes across the Xizangan Plateau revealed using a large-scale automated assessment approach. Science Bulletin, 64(7): 435−445. DOI：10.1016/j.scib.2019.03.011.

Ashraf A, Naz R, Roohi R. 2012. Glacial lake outburst flood hazards in Hindukush, Karakoram and Himalayan Ranges of Pakistan: Implications and risk analysis. Geomatics, Natural Hazards and Risk, 3(2): 113−132. DOI: 10.1080/19475705.2011.615344.

Chen NS, Wang Z, Tian SF, et al. 2019b. Study on debris flow process induced by moraine soil mass failure. Quaternary Sciences, 39(5): 1235−1245. (in Chinese)

Chen Q, Guo XF. 2019c. Soil structure and in-site shear test of moraine soil near the Xingkang Bridge over the Daduhe River in Luding. Hydrogeology and Engineering Geology,

46(4): 126−133.

Chen T. 2019a. Impacts of cyclic F-T on strength properties of coarse-grained soils and slope stability of mine dump. MS. Theis. Lanzhou. Lanzhou University of Technology.

Cui P, Ge YG, Li SJ, et al. 2022. Scientific challenges in disaster risk reduction for the Sichuan–Xizang Railway. Engineering Geology, 309: 106837. DOI：10.1016/j.enggeo.2022.106837.

Fang XD, Huang RQ. 2013. Physical and mechanical properties of typical moraine soil on the Qinghai-Xizang Plateau. Journal of Engineering Geology, 21(1): 123−128. (In Chinese)

Feng XL, Li ZR, Jiang MG, et al. 2024. Experimental study of soil erosion on moraine-consolidated slopes under heavy rainfall. Heliyon, 10(5): e26721. DOI：10.1016/j.heliyon.2024.e26721.

Gao B, Zhang JJ, Wang JC, et al. 2019. Formation mechanism and disaster characteristics of debris flow in the Tianmo gully in Xizang. Hydrogeology and Engineering Geology, 46(5): 144−153.

Guo XF, Cheng Q, Zhang LL, et al. 2022. Large-scale in situ tests for shear strength and creep behavior of moraine soil at the Dadu River bridge in Luding, China. International Journal of Geomechanics, 22(5): 04022053. DOI：10.1061/(asce)gm.1943-5622.0002362.

Guo XF, Xing XF, Wang ZH, et al. 2023. Compression characteristic and creep behavior of moraine soil at xingkang bridge, west Sichuan, China. Journal of Earth Science, 34(4): 1272−1279. DOI：10.1007/s12583-022-1800-4.

Han Y, Wang Q, Wang N, et al. 2018. Effect of freeze-thaw cycles on shear strength of saline soil. Cold Regions Science and Technology, 154: 42−53. DOI：10.1016/j.coldregions.2018.06.002.

Jiang Y, Lu XS, Liu ZM, et al. 2024. Experimental study on the engineering properties and failure mechanism of moraine in Southeast Xizang under freeze–thaw cycles conditions. Engineering Failure Analysis, 163: 108551. DOI：10.1016/j.engfailanal.2024.108551.

Klimeš J, Novotný J, Novotná I, et al. 2016. Landslides in moraines as triggers of glacial lake outburst floods: Example from Palcacocha Lake (Cordillera Blanca, Peru). Landslides, 13(6): 1461−1477. DOI：10.1007/s10346-016-0724-4.

Lebourg T, Riss J, Pirard E. 2004. Influence of morphological characteristics of heterogeneous moraine formations on their mechanical behaviour using image and statistical analysis. Engineering Geology, 73(1−2): 37−50. DOI: 10.1016/j.enggeo.2003.11.004.

Liu JK, Chang D, Yu QM. 2016. Influence of freeze-thaw cycles on mechanical properties of a silty sand. Engineering Geology, 210: 23−32. DOI：10.1016/j.enggeo.2016.05.019.

Liu JK, Zhang JJ, Gao B, et al. 2019. An overview of glacial lake outburst flood in Xizang, China. Journal of Glaciology and Geocryology, 41(6): 1335−1347.

Luo F, Liu EL, Zhu ZY. 2019. A strength criterion for frozen moraine soils. Cold Regions Science and Technology, 164: 102786. DOI：10.1016/j.coldregions.2019.102786.

Lv S, Wang N, Hu MJ, Shen JH. 2017. Current status, problems and future trends of the research on engineering properties of moraine soil. Journal of Engineering Geology, 19: 307−312.

Neupane R, Chen HY, Cao CR. 2019. Review of moraine dam failure mechanism. Geomatics, Natural Hazards and Risk, 10(1): 1948−1966. DOI: 10.1080/19475705.2019.1652210.

Palamakumbura R, Finlayson A, Ciurean R, et al. 2021. Geological and geomorphological influences on a recent debris flow event in the Ice-scoured Mountain Quaternary domain, western Scotland. Proceedings of the Geologists' Association, 132(4): 456−468. DOI：10.1016/j.pgeola.2021.05.002.

Pan L, Wei XL, Zhang YF, et al. 2017. Influence of initial water content on glacial debris flow triggering process. Journal of Soil and Water Conservation, 31(6): 116−122. (in Chinese) DOI：10.13870/j.cnki.stbcxb.2017.06.020.

Peng DL, Zhang LM, Jiang RC, et al. 2022. Initiation mechanisms and dynamics of a debris flow originated from debris-ice mixture slope failure in southeast Xizang, China. Engineering Geology, 307: 106783. DOI：10.1016/j.enggeo.2022.106783.

Qiu EX, He QL, Chen QL, et al. 2023. Influence of freeze–thaw cycles on mechanical properties

of moraine soils. Transportation Geotechnics, 42: 101097. DOI：10.1016/j.trgeo.2023.101097.

Qu YP, Xiao J, Pan YW. 2018. Preliminary analysis on formation conditions of glacier debris flow in Southeast Xizang—a case of glacial debris flow in Tianmo Gully. Water Resources and Hydropower Engineering, 49(12): 177−184. (in Chinese) DOI：10.13928/j.cnki.wrahe.2018.12.024.

Shen YJ, Wei X, Zhang L, et al. 2022. Hydrothermal migration of moraine soil and the mechanism of ice accumulation and frost swelling in alpine-cold mountain region. Journal of Engineering Geology, 30(5): 1450−1465. (in Chinese) DOI：10.13544/j.cnki.jeg.2022-0449.

Sokolov VN, Razgulina OV, Yurkovets DI, et al. 2007. Quantitative analysis of pore space of moraine clay soils by SEM images. Journal of Surface Investigation. X-Ray, Synchrotron and Neutron Techniques, 1(4): 417−422. DOI: 10.1134/S1027451007040106.

Wang D, Yang CS, Ma W, et al. 2020. The status and review of frozen fringe in freezing soils. Journal of Glaciology and Geocryology, 42(4): 1195−1201. (in Chinese)

Wang Q, Wang JP. 2000. A study on fractal of porosity in the soils. Chinese Journal of Geotechnical Engineering, 22(4): 496−498. (In Chinese)

Wang YK, Liu XL, Zhang XL, et al. 2023. Dynamic response characteristics of moraine-soil slopes under the combined action of earthquakes and cryogenic freezing. Cold Regions Science and Technology, 211: 103854. DOI：10.1016/j.coldregions.2023.103854.

Zhang LH, Shi YJ, Yang CS, et al. 2024. Water accumulation unrelated to ice segregation near the freezing front during soil freezing: Implications for frost heave in high-speed railway embankments and ground ice formation. Catena, 243: 108189. DOI：10.1016/j.catena.2024.108189.

Zhao W, Wang XJ, Xu ZX, et al. 2021. Experimental study on natural evolution characteristics of coarse-grained soil slope in seasonal frozen soil region. Journal of Engineering Geology, 29(5): 1497−1506. (in Chinese) DOI：10.13544/j.cnki.jeg.2020-174.

Zhou GGD, Roque PJC, Xie YX, et al. 2020. Numerical study on the evolution process of a geohazards chain resulting from the Yigong landslide. Landslides, 17(11): 2563−2576. DOI：10.1007/s10346-020-01448-w.

Zhou JQ, Zhu WY, Li QL, et al. 2023. Characterization of thermal-hydraulic coupling behavior for moraine soil with ice inclusions in a warming environment. Water Resources Research, 59(12): e2022WR033852. DOI：10.1029/2022WR033852.

Zhou Z, Li F, Yang H, et al. 2021. Orthogonal experimental study of soil–rock mixtures under the freeze–thaw cycle environment. International Journal of Pavement Engineering, 22(11): 1376−1388. DOI：10.1080/10298436.2019.1686634.